ENCIT 2018

ABCM Associação Brasileira de Engenharia e Ciências Mecânicas

17th Brazilian Congress of Thermal Sciences and Engineering
November 25th-28th, 2018, Águas de Lindóia, SP, Brazil

ENCIT-2018-0064
STABILITY ANALYSIS OF LONG INTERFACIAL WAVES IN GAS-LIQUID PIPE FLOW USING A LEVEL-SET APPROACH

Matheus A. S. A. Dias
Daniel Rodríguez
Laboratory of Theoretical and Applied Mechanics (LMTA), Graduate Program in Mechanical Engineering (PGMEC), Mechanical Engineering Department, Universidade Federal Fluminense, Niteroi, RJ 24210-240, Brazil.
matheus.a.s.a.dias@hotmail.com, danielrodriguez@id.uff.br

Anis A. Ayati
Department of Mathematics, University of Oslo, N-0316 Oslo, Norway
awalaa@math.uio.no

Abstract. *Linear stability analysis is used to model and predict the main characteristics of long interfacial waves appearing spontaneously in air-water flow along a very long pipe of circular cross-section. Reynolds numbers are high enough to ensure that the air phase is in turbulent regime. A local stability analysis for two-phase flows based on the Level Set approach is applied, that only requires of the mean turbulent field as external data. Data from a series of companion experiments using hot-wire, conductance probes and a novel PIV which measures simultaneously the two phases is used here to provide the mean flow and to compare the predictions of the stability calculations for the interfacial waves. Linear stability analysis is found to predict well the dominant wavelengths and frequencies, as well as the spatial structure of the velocity fluctuations, for this kind of long gravitational waves.*

Keywords: *Multiphase flow, Flow instability, Turbulence, Interfacial waves*

1. INTRODUCTION

Technological problems in which two or more fluids flow concurrently along pipes are present in many fields of engineering, like chemical process or oil extraction. The ability of predicting the formation of potentially harmful long gravitational waves, precursors of the pattern transition towards an intermittent regime, is of prime importance in the design and operation of complex transport lines. Methodologies used presently in industrial applications rely on the so-called one-dimensional two-fluids model for the simulation of these kind of flows (Taitel and Dukler (1976)). The underlying simplification is the assumption of uniform velocity within each fluid phase, leading to section-averaged equations only dependent on the longitudinal direction and time. In order to close the system of equations, friction factors are introduced in the equations that require extensive experimental calibration for all expected working conditions. The success of the one-dimensional two-fluids approach in spatio-temporal simulations presents, however, the well-known difficulty in the prediction of flow pattern transitions. Attempts of implementing linear stability analysis based on the two-fluid method have been proved unreliable, in spite of few decades of calibrations and refining (Lin and Hanratty (1986); Barnea and Taitel (1993)).

On the other hand, methods derived from first-principles for understanding the physical processes associated with interfacial instabilities, like those presented by Renardy (1987) or Boomkamp and Miesen (1997), have not been applied in the same degree as the one-dimensional two-fluids model, due to their higher computational expenditure. Instead of resorting to the cross-sectional averaged equations, these methods consider the complete momentum and mass conservation equations, together with appropriate boundary and interfacial conditions, thus retaining the pertinent advection, flow shear, viscous dissipation, gravity, interfacial tension and pressure diffusion. As a result, a linear stability analysis based on the complete equations provides not only the dominant frequencies and wavelengths for interfacial waves, but also their spatial structure and underlying physics. On the other hand, they require a more detailed information of the underlying flow in which the interfacial wave develop. Recent publications (Kaffel and Riaza (2015); Barmak *et al.* (2016)) successfully applied this methodology to the prediction of interfacial waves and pattern transition of laminar flows in channels. Literature is scarce in applications of this methodology to gravity-stratified flows in circular pipes, and/or turbulent flows.

This work addresses the linear modal instability of air-water flow along long pipes of circular cross section, with superficial velocities of $O(0.1)$m/s and $O(1)$m/s for the liquid and gas phases respectively, and an inner diameter of 10 cm. Under these conditions, the two phases are turbulent and plane interfacial waves can develop without an explicit external excitation. The linear stability problem based on the Level Set approach introduced in the recent years by

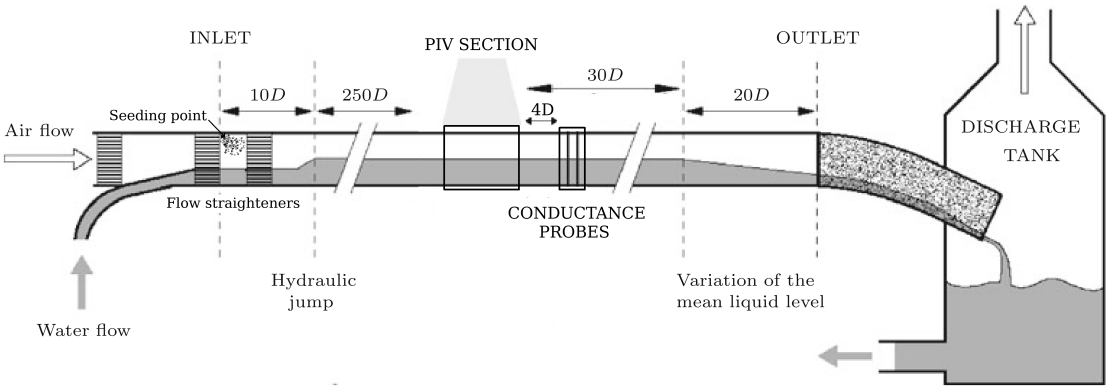

Figure 1. Schematic view of the experimental setup.

Rodríguez (2015); Rodríguez and Gennaro (2016) and Marins *et al.* (2017) is applied on the vertical middle section of the pipe, in order to analyze a quasi-plane configuration in which the pipe curvature and secondary flows are neglected. Data from a comprehensive experimental campaign combining hot-wire, conductance probes and particle image velocimetry (Ayati *et al.* (2014, 2015, 2016)) are be used to inform the instability analysis with the correct turbulent mean flow, and to compare the predictions of the analysis with the measured interfacial waves.

The rest of the paper is organized as follows. The experimental set-up and data processing is briefly outlined in section 2. Section 3describes the formulation of the linear stability problem based on the level set approach. Section 4present the results of the stability analysis. Some conclusions are drawn in section 5.

2. EXPERIMENTAL SET-UP AND DATA PROCESSING

Experiments were conducted at the Hydrodynamic Laboratory at the University of Oslo. The facilities dispose a two-phase flow loop consisting of a 31m long acrylic pipe with inner diameter $D^* = 0.1$m, i.e. yielding a length-to-diameter ratio of 310. Ayati *et al.* (2015) showed that this pipe length is sufficient to achieve statistically convergent interfacial flow patterns and velocity profiles. A schematic view of the pipe-loop is shown in Fig. 1.

Air and water at atmospheric pressure were introduced at the loop inlet using a frequency-regulated fan and pump, respectively. Reynolds numbers can reach up to 50×10^3 for air and 25×10^3 for water. The mass flow rates of water and air were measured with an Endress Hauser Promass and an Emerson MicroMotion Coriolis flow meter with 0.2% and 0.05% of maximal measured values in accuracy, respectively. The static pressure drop was measured between two taps separated by 12.4m using a SMAR LD 301 differential gauge ($\pm 0.2\%$ in accuracy).

The main experimental set-up consisted of Particle Image Velocimetry (PIV), conductance probes (CP) and hot-wire anemometry (HW). The PIV section, placed approx. $260D^*$ downstream of the pipe inlet, made use of two 16bit PCO4000 cameras and one high power double-pulsed Nd:YAG laser of 135 mJ in order to provide simultaneous planar measurements of air and water velocity fields at the pipe center-plane. Each camera recorded 1000 images with a pixel resolution of 4008×2672 (streamwise×wall-normal direction). The interrogation process of the recorded PIV realizations was carried out using Digiflow (Dalziel Research Partners) with interrogation widows of 64×32 pixels and 50% overlap. This choice of window size and overlapping domain led velocity fields containing 124×167 vectors and a spatial dynamic range (SDR) of 63×84. The air-phase was seeded with small water droplets ($\bar{d} < 10\mu s$) which were injected at the pipe inlet, while the water-phase was seeded with commercial polyamide particles ($\bar{d} = 50\mu s$). A through assessment of the accuracy of this method, including the passiveness of the air tracer particles was outlined by Ayati *et al.* (2014).

Furthermore, the CP section was placed 4D downstream of the PIV section and consisted of two double-wire probes made of platina. Each probe provided interface elevation measurements with high temporal resolution ($Fs = 500Hz$). The probes were placed at the pipe center and separated by 6cm, providing wave celerity measurements through cross-correlation in addition to local wave statistics. Finally, a Dantec Dynamics miniature hot-wire X-probe (55P63) was placed approximately 20D upstream of the PIV section. The probe was mounted to a motorized transverse system which allowed it to measure air fluctuations along the pipe vertical center-line. The sampling frequency was set to 5000Hz, slightly above the cut-off frequency of 4200Hz, which is related to sensor length (1.25mm). For more details about the flow loop as well as the experimental techniques, see Ayati *et al.* (2014, 2015, 2016).

3. MODELING OF THE INTERFACIAL WAVES

The mathematical model for the confined two-phase flow is based on the complete Navier-Stokes equations in differential form. A single-fluid method along with an interface-capturing Level Set approach is used here to describe the fluid

motion, as described next.

Equations are non-dimensionalized using the following magnitudes: the pipe inner diameter D^* as characteristic length; a characteristic velocity U^* (chosen as 1 m/s to ease the comparison of different cases); the density and molecular viscosity in the lighter phase 1, ρ_1^* and μ_1^*; a characteristic advection time D^*/U^*; and the dynamic pressure $\rho_1^* U^{*2}$. Denoting the acceleration of gravity by g^* and the surface tension coefficient between the two phases by σ^*, the following dimensionless quantities are formed:

$$\chi = \frac{\rho_2^*}{\rho_1^*}, \quad \eta = \frac{\mu_2^*}{\mu_1^*}, \quad Re = \frac{\rho_1^* U^* D^*}{\mu_1^*}, \quad We = \frac{\rho_1^* U^{*2} D^*}{\sigma^*} \quad \text{and} \quad Fr = \frac{U^*}{\sqrt{g^* D^*}}. \tag{1}$$

In this dimensionless form, the momentum and mass conservation equations can be written as

$$\rho \frac{\partial \mathbf{v}}{\partial t} + \rho \mathbf{v} \cdot \nabla \mathbf{v} = -\nabla p + \frac{1}{Re} \nabla \cdot (2\mu \mathbf{D}) + \frac{1}{We} \mathbf{T} + \frac{\rho}{Fr^2} \mathbf{g}, \quad \text{and} \quad \nabla \cdot \mathbf{v} = 0, \tag{2}$$

where $\mathbf{D} = (\partial u_i/\partial x_j + \partial u_j/\partial x_i)/2$ is the velocity gradient tensor, $\mathbf{T}$ is a volume force modeling the surface tension and $\mathbf{g}$ is the unitary vector pointing in the direction of gravity.

The Level Set method (Sussman *et al.* (1994)) is employed here in order to capture the fluid interface and track its deformation. A scalar level function ϕ is defined such that $\phi = 0$ at the interface, $\phi > 0$ at phase 1 and $\phi < 0$ at phase 2. The ϕ function is governed by the advection equation

$$\frac{\partial \phi}{\partial t} + \mathbf{v} \cdot \nabla \phi = 0. \tag{3}$$

After introduction of ϕ, the density and viscosity spatial distributions are expressed as

$$\rho = H(\phi) + \chi(1 - H(\phi)), \quad \text{and} \quad \mu = H(\phi) + \eta(1 - H(\chi)), \tag{4}$$

where H is the Heaviside function.

Provided that $\phi = 0$ defines the interface location, the interface local normal vector, curvature and surface tension are determined as

$$\mathbf{n} = -\frac{\nabla \phi}{|\nabla \phi|}, \qquad \kappa(\phi) = \nabla \cdot \left(\frac{\nabla \phi}{|\nabla \phi|} \right), \quad \text{and} \quad \mathbf{T} = \kappa(\phi)\delta(\phi)\mathbf{n} = -\delta(\phi) \nabla \cdot \left(\frac{\nabla \phi}{|\nabla \phi|} \right) \frac{\nabla \phi}{|\nabla \phi|}, \tag{5}$$

where the Dirac delta function δ has been used. The fluid flow described by equations (2), and (3) is represented in vector form as $\mathbf{q} = [\mathbf{v}\ p\ \phi]^T$, and in the most general case is a function of the three spatial directions (x denoting the axial direction, y the vertical and z the transversal ones) and time t.

3.1 Linear Stability Analysis

This paper aims to model the long gravitational waves naturally appearing on turbulent gas-liquid flow as instabilities of the time-averaged flow. Following Reynolds decomposition, the flow is divided into a time-independent *mean* flow $\bar{\mathbf{q}}$ and a fluctuation component $\mathbf{q}'$:

$$\mathbf{q} = \bar{\mathbf{q}}(\mathbf{x}) + \mathbf{q}'(\mathbf{x}, t). \tag{6}$$

The mean flow $\bar{\mathbf{q}}$ is measured experimentally, as briefly described in section 2. Upon substitution of (6) in the governing equations (2), and (3), and linearization about the mean flow, a system of homogeneous partial-differential equations is obtained that governs the behavior of disturbances of infinitesimal amplitude. This work assumes that the principal transversal section of the mean flow (i.e. the vertical plane at the middle pipe section, which is measured in the experiments) dictates, as a first approximation, the properties of the interfacial waves. Together with the fully-developed flow assumption, the former hypothesis implies that the mean flow only depends on the vertical direction, $\mathbf{q}(y)$. Consequently and without loss of generality, the modal form

$$\mathbf{q}'(x, y, t) \sim \hat{\mathbf{q}}(y) \exp\left[\mathrm{i}(\alpha x - \omega t)\right] \tag{7}$$

is introduced for the disturbances. Substituting (7) on the governing equations and reordering terms, the generalized eigenvalue problem for the modal instability analysis is obtained in the form

$$\mathrm{i}\omega \mathbf{B} \hat{\mathbf{q}} = \mathbf{A}(\alpha, Re, We, Fr, \bar{\mathbf{q}}) \hat{\mathbf{q}}. \tag{8}$$

For given parameters Re, We, Fr and mean flow $\bar{\mathbf{q}}(y)$, the matrix eigenvalue problem (8) relates the values of the streamwise wavenumber α and the frequency ω for different families of possible linear waves.

In the temporal instability analysis, α is a real value corresponding to a streamwise periodicity length, and the eigenvalues are complex ω values, the real part ω_r of which corresponds to the circular frequency and the imaginary part ω_i to the temporal growth rate. If $\omega_i > 0$ for one eigenmode, then its amplitude will grow with time and the base flow is unstable. Stability of the base flow requires that $\omega_i < 0$ for all the eigenmodes.

Table 1. Parameters characterizing the different experimental cases. U^*_{max} is the peak mean velocity, attained in the gas phase. h is the liquid hold-up measured from the pipe bottom, dimensionalized with the inner diameter D^*; the values given for h correspond to the pixel position closer to the mean interface in the PIV measurements.

Case	U^*_{sA} [m/s]	U^*_{sW} [m/s]	U^*_{max} [m/s]	h [-]	sub-regime
A1	0.08	1.09	2.579	0.3581	Smooth
A2	0.08	1.27	2.867	0.3581	Smooth
A3	0.08	1.54	3.391	0.3488	Transition to 2D waves
A4	0.09	1.74	3.850	0.3606	Transition to 2D waves
B1	0.10	1.54	3.758	0.3646	Transition to 2D waves
B2	0.10	1.77	4.025	0.3704	2D waves
B3	0.10	2.03	4.456	0.3704	2D waves
B4	0.10	2.29	4.926	0.3876	2D waves

3.2 Numerical Methods

The linear stability eigenvalue problem (8) is discretized using sixth-order finite differences. For numerical reasons, the Heaviside and Dirac's functions are replaced in the computations by smoothed functions, following Sussman *et al.* (1994). The width of the resulting smoothed interface is chosen to be twice the grid spacing. The eigenvalue problem (8) is solved using an in-house implementation of the shift-and-invert Arnoldi algorithm. This Krylov's subspace iteration allows the computation of an arbitrarily large window of the eigenspectrum at a small fraction of the cost of alternatives like the QZ algorithm.

Further information on the linear stability analysis based on the Level Set approach can be found in Rodríguez (2015); Rodríguez and Gennaro (2016); Marins *et al.* (2017).

4. RESULTS

The co-flowing air-water experimental set-up described in section 2.corresponds to the density and viscosity ratios $\chi = 833$ and $\eta = 52$, respectively. Taking the characteristic velocity as $U^* = 1$ m/s, the Reynolds, Weber and Froude numbers result $Re = 6.67 \cdot 10^3$, $We = 1.701$ and $Fr = 1.01$. Different experimental conditions were considered, characterized by the superficial velocity of the air and water phases, U^*_{sA} and U^*_{sW}. Table 1 summarizes the different cases. A smooth interface is observed for the lower superficial velocities of water and air. As they are increased, the flow undergoes a transition to organized two-dimensional waves, that first appear in a disorganized manner. For the higher speeds considered here, the two-dimensional wave pattern is observed in a robust manner. Frequency spectra (not shown here, cf. Ayati *et al.* (2015)) of the conductance probes present two well-defined peaks for cases in which two-dimensional waves are observed, the one of lower amplitude being the harmonic of the second one. For case B3 (U^*_{sA} =0.1 m/s, U^*_{sW} =2.03 m/s), the peak frequency is $f \approx 3.8$ Hz. The average wavelength of the interfacial waves observed in the experiments is $\lambda_x \approx 2.3D^*$.

Figures 2(a-c) show the mean turbulent flow and the rms of the streamwise and transversal velocity fluctuations, measured using the two-phase PIV for case B3. The lighter grey area denotes the location of the interface; due to the finite-amplitude, temporal oscillations of the interface, a single location cannot be defined for the interface but rather a region. The 2F-PIV presents limitations in recovering the details of the velocity field in the vicinity of the moving interface. This behavior is mimicked in the stability calculations by adapting the finite-thickness interface region of the Level Set method to coincide with the "diffuse" experimental interface. The darker grey area in the figures denotes a region where light reflections stemming from the pipe walls contaminate the PIV measurements. Prior to its use as base flow in the stability calculations, the experimental mean flow needs to be processed. The vertical coordinate is adjusted and rescaled. A cubic spline is used to produce a smooth interpolation in the region of the reflection. First and second order derivatives of the mean flow $\mathrm{d}\bar{u}/\mathrm{d}y$ and $\mathrm{d}^2\bar{u}/\mathrm{d}y^2$, required in the stability analysis, are computed numerically in the same mesh used in the computations to ensure consistency of the numerics.

Linear stability results identify several families of instability eigenmodes, as discussed by Marins *et al.* (2017). For the turbulent mean flows analyzed here, only the isolated eigenmode corresponding to the interfacial instability is temporally amplified, which occurs for a very large range of streamwise wavenumbers. The solution of the eigenvalue problem 8 for the dominant wavenumber $\alpha = 2.77$ in experiments recovers an unstable eigenmode with eigenvalue $\omega = 2.108 + \mathrm{i}0.016$, corresponding to a frequency of $f^* \approx 3.4$ Hz, in good agreement with the CP spectra. Figures 2(d-e) show the streamwise and vertical components of the eigenfunction corresponding to this leading eigenmode. Compared to the fluctuation's rms in Figs. 2(b-c), it can be observed that the most salient features of the interfacial waves are reproduced by the eigenmode: (i) the sharp peak streamwise velocity in the air phase, in the vicinity of the interface, that decays fast towards the inner

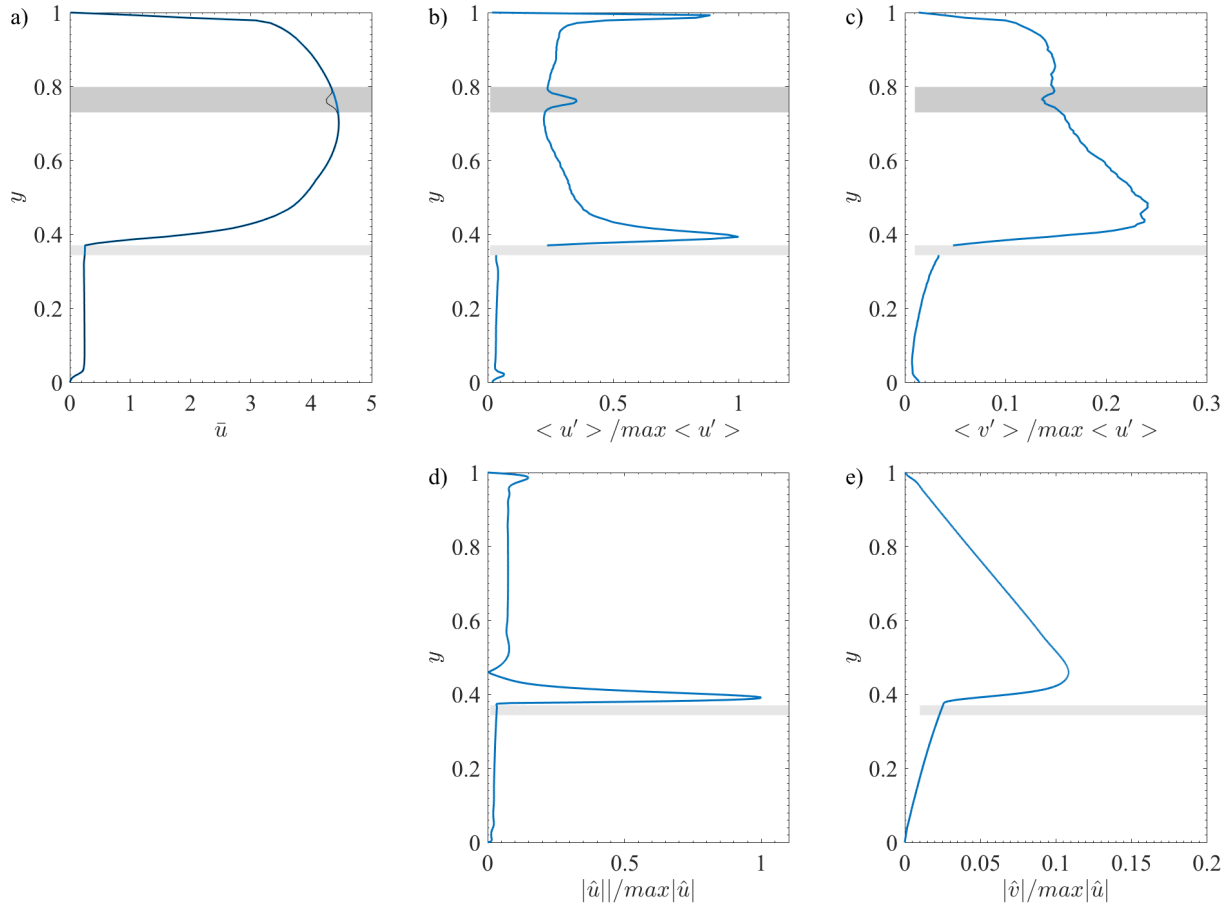

Figure 2. Turbulent mean flow $\bar{u}$ (a), streamwise rms velocity $< u' >$ (b) and vertical rms velocity $< v' >$ (c) measured using 2F-PIV for the case B3 (U^*_{sA} =0.1 m/s, U^*_{sW} =2.03 m/s). Black line in (a) corresponds to the measurement and blue one to the corrected one, used in the stability analysis. Streamwise (d) and vertical (e) velocity components of the eigenfuction corresponding to the interfacial instability eigenmode in the linear stability analysis, corresponding to the dominant wavenumber observed in the experiments. ($\alpha = 2.77, \omega = 2.108 + \mathrm{i}0.016$).

of the air phase; (ii) a peak in the vertical velocity in the air phase near the interface that decays nearly linearly on y; (iii) smaller relative velocity amplitudes in the two components in the water phase, that decay away from the interface towards the wall. Differences in the air phase can be attributed to flow oscillations unrelated to the long interfacial waves, which are dominant near the walls due to the turbulent boundary layer, and to components of the interfacial waves of wavelength different to the dominant one.

Interestingly, the dominant wavenumber in the experiments is very different from the most unstable one in the linear stability analysis. The dependence of the circular frequency and growth rate on the wavenumber is shown in figure 3 for a representative case. These results are in very good agreement with analogous analyses for laminar two-phase flow in channels Kaffel and Riaza (2015); Barmak *et al.* (2016). Two-dimensional reconstructions of the modal perturbations corresponding to the leading wavenumber in experiments and predicted by the linear stability analysis are shown respectively in figures 4 and 5. The streamwise domain is the same in the two case and vertical and horizontal axes are in the same scale. The wave shown in figure 4 exhibits the typical characteristics of long waves or gravitational waves reported in the literature. The corresponding wavelength is $\sim$ 2.77 times the pipe diameter. The peak streamwise disturbance velocity is approximately tenfold larger than the vertical one. While the streamwise component is strongly localized around the interface, the vertical component extends over the complete gas phase, representing a global periodic compression and expansion of this phase. On the other hand, the large wavenumber eigenmode (figure 5)found to be most unstable can be related to capillarity waves: both streamwise and vertical velocity components are of the same order and are localized in the vicinity of the interface. The associated wavelength is ~ 0.2 times the pipe diameter. Analogous results are found for the other flow conditions in table 1, and not shown here.

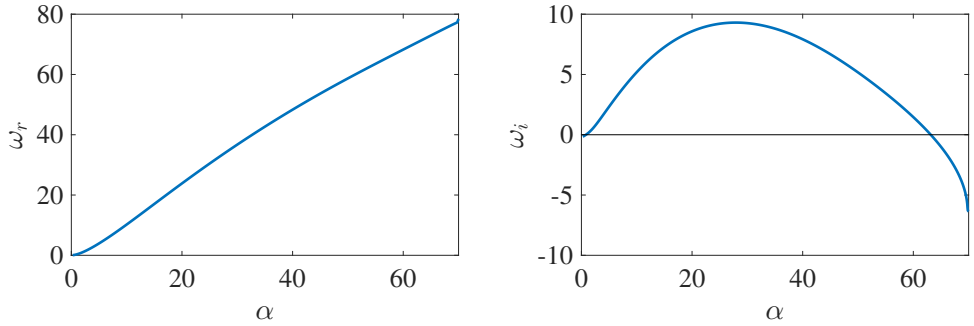

Figure 3. Interfacial instability eigenmode for case B3 (U^*_{sA} =0.1 m/s, U^*_{sW} =2.03 m/s). Circular frequency (left) and growth rate (right) as a function of the streamwise wavenumber.

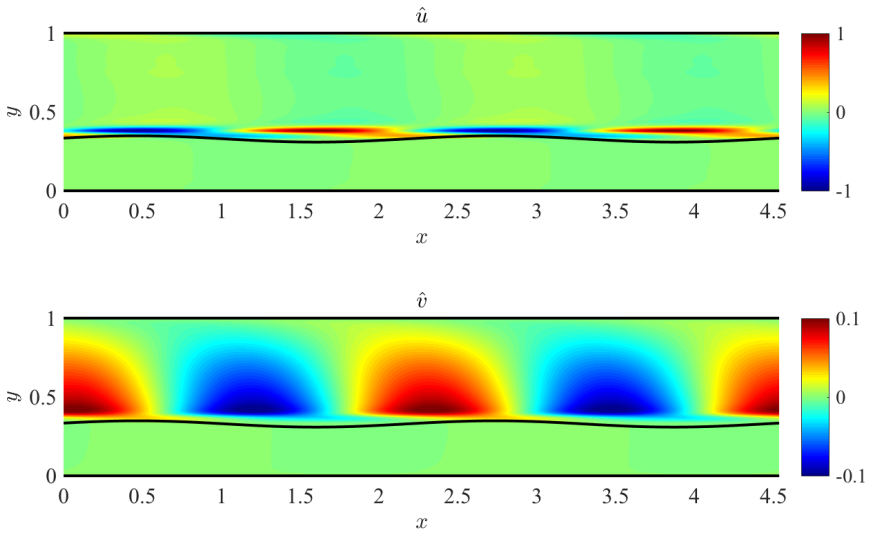

Figure 4. Streamwise (top row) and vertical (bottom row) velocity components of the interfacial eigenmode for case B3 (U^*_{sA} =0.1 m/s, U^*_{sW} =2.03 m/s), corresponding the leading streamwise wavenumber in the experiments ($\alpha = 2.77$) and as predicted by the linear stability analysis ($\alpha = 29.7$).

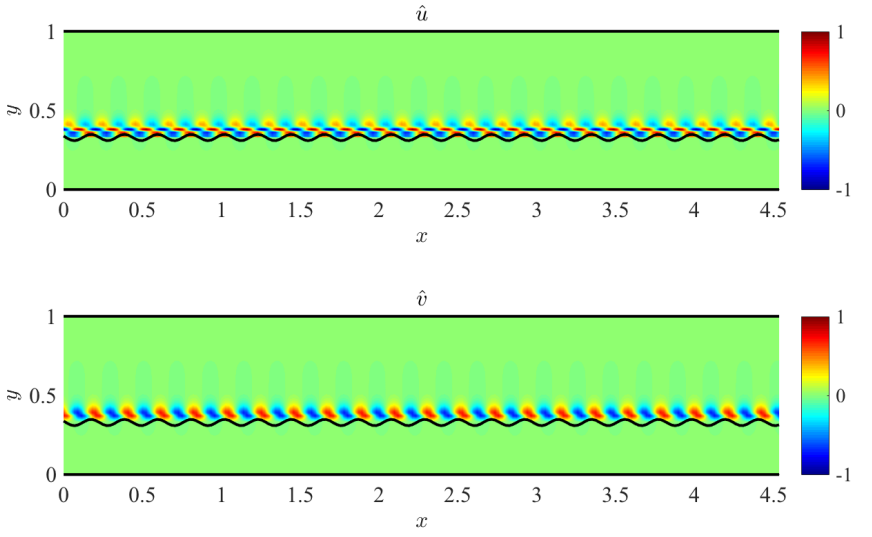

Figure 5. Streamwise (top row) and vertical (bottom row) velocity components of the interfacial eigenmode for case B3 (U^*_{sA} =0.1 m/s, U^*_{sW} =2.03 m/s), corresponding the leading streamwise wavenumber predicted by the linear stability analysis ($\alpha = 29.7$).

5. CONCLUSIONS

This paper presented results of a linear stability analysis of air-water flow along a circular pipe. The mean turbulent velocity profile measured at the central vertical section of the pipe using PIV was used as the base flow, invoking the parallel-flow assumption and neglecting the lateral effects. A formulation of the local instability problem in the temporal framework based on the Level Set approach was used to the two-phase flow. No additional modeling was done to introduce turbulent effects, on the idea that most of the nonlinear effects associated with the turbulence are already considered implicitly with the use of the turbulent mean flow.

The linear stability analysis recovers at most a single unstable eigenmode at each wavenumber, which is associated with the interface. Wall eigenmodes, associated with viscous instability mechanisms remained stable for all cases, which agrees with modal analysis of channel and boundary-layer single-phase flows. The interfacial eigenmode was found to be unstable for a very large range of wavenumbers, while visual inspection of the corresponding eigenfunction illustrates that this eigenmode transitions from one physical behavior to another. For low wavenumbers ($\alpha \approx 2.77$), long or gravitational waves are recovered which agree well with the dominant interfacial waviness measured in the experiments. However, the growth rate for these wavenumbers are low compared to that at $\alpha \approx 29.7$, for which the maximum linear modal amplification is attained. At the latter conditions, the eigenfunction resembles capillary waves.

Our results agree qualitatively with previous works in the literature reporting modal analyses of laminar and turbulent two-phase flow in channels, including the apparent controversy between the long waves observed experimentally and the most unstable capillary waves recovered by the theory. Possible explanations require the consideration of non-linear effects and possible interactions between interfacial instabilities of very different wavelengths.

6. ACKNOWLEDGMENTS

The authors acknowledge funding from CNPq (grants 405144/2016-4, 305512/2016-1), SIU/CAPES joint program UTFORSK2016 (grant UTF.2016-CAPES-SIU/10012), and FAPERJ (grants 200003, 223669).

7. REFERENCES

Ayati, A., Kolaas, J., Jensen, A. and Johnson, G., 2014. "A PIV investigation of stratified gasâĂŞliquid flow in a horizontal pipe". *International Journal of Multiphase Flow*, Vol. 61, pp. 129 – 143.

Ayati, A., Kolaas, J., Jensen, A. and Johnson, G., 2015. "Combined simultaneous two-phase {PIV} and interface elevation measurements in stratified gas/liquid pipe flow". *International Journal of Multiphase Flow*, Vol. 74, pp. 45 – 58.

Ayati, A., Kolaas, J., Jensen, A. and Johnson, G., 2016. "The effect of interfacial waves on the turbulence structure of stratified air/water pipe flow". *International Journal of Multiphase Flow*, Vol. 78, pp. 104 – 116. ISSN 0301-9322.

Barmak, I., Gelfgat, A., Vitoshkin, H., Ullmann, A. and Brauner, N., 2016. "Stability of stratified two-phase flows in horizontal channels". *Phys. Fluids*, Vol. 28, p. 044101.

Barnea, D. and Taitel, Y., 1993. "Kelvin-Helmholtz instability criteria for stratified flow: viscous versus non-viscous (inviscid) approaches". *Int. J. Multiphase Flow*, Vol. 19, No. 4, pp. 639–649.

Boomkamp, P.A.M. and Miesen, R.H., 1997. "Classification of instabilities in parallel two-phase flow". *Int. J. Multiphase Flow*, Vol. 22, No. Suppl, pp. 67–88.

Kaffel, A. and Riaza, A., 2015. "Eigenspectra and mode coalescence of temporal instability in two-phase channel flow". *Phys. Fluids*, Vol. 27, p. 042101.

Lin, P. and Hanratty, T., 1986. "Prediction of the Initiation of Slugs with Linear Stability Theory". *Int. J. Multiphase Flow*, Vol. 12, No. 1, pp. 79–98.

Marins, B.S., Jotkar, M.R. and Rodríguez, D., 2017. "Two-phase flow stability analysis using a level set approach". 24th ABCM International Conference of Mechanical Engineering - COBEM, December 3-8th, Curitiba, PR, Brazil.

Renardy, Y., 1987. "Then thin-layer effect and interfacial stability in a two-layer Couette flow with similar liquids". *Physics of Fluids*, Vol. 30, No. 6, pp. 1627–1637.

Rodríguez, D., 2015. "A novel modeling method for the interfacial instability of immiscible fluids along ducts". 23rd ABCM International Conference of Mechanical Engineering - COBEM, December 6-11th, Rio de Janeiro, RJ, Brazil.

Rodríguez, D. and Gennaro, E.M., 2016. "Development of a new approach for the prediction of pattern transition of two-phase stratified flow in ducts and pipes". 16th Brazilian Congress of Thermal Sciences and Engineering - ENCIT, November 7-10th, Vitória ES, Brazil.

Sussman, M., Smereka, P. and Osher, S., 1994. "A level set approach for computing solutions to incompressible two-phase flow". *J. Comp. Phys.*, Vol. 114, pp. 146–159.

Taitel, Y. and Dukler, A., 1976. "A Model for predicting flow Regime transitions in horizontal and near horizontal gas-liquid flow". *A. I. Ch. E.*, Vol. 22, pp. 47–55.

8. RESPONSIBILITY NOTICE

The authors are the only responsible for the printed material included in this paper.